Understanding and Improving the Performance of Constructive Interference Using Destructive Interference in WSNs

Rao, Vijay S.; Prasad, R. Venkatesha; Prabhakar, T. V.; Sarkar, Chayan; Koppal, Madhusudan; Niemegeers, Ignas

DOI
10.1109/TNET.2019.2893597

Publication date
2019

Document Version
Final published version

Published in
IEEE/ACM Transactions on Networking

Understanding and Improving the Performance of Constructive Interference Using Destructive Interference in WSNs

Vijay S. Rao, *Member, IEEE*, R. Venkatesha Prasad, *Senior Member, IEEE, ACM*, T. V. Prabhakar, *Member, IEEE*, Chayan Sarkar, *Member, IEEE*, Madhusudan Koppal, and Ignas Niemegeers, *Member, IEEE*

***Abstract*— The constructive interference (CI) phenomenon has been exploited by a number of protocols for providing energy-efficient, low-latency, and reliable data collection and dissemination services in wireless sensor networks. These protocols consider CI to provide highly reliable packet delivery. This has attracted attention to understand the working of CI; however, the existing works present inconsistent views. Furthermore, these works do not study in the real-world settings where the physical conditions of deployment and unreliable wireless channels also impact the performance of CI. Therefore, we study the phenomenon of CI, considering a receiver's viewpoint and analyze the parameters that affect CI. We validate our arguments with results from extensive and rigorous experimentation in real-world settings. This paper presents comprehensive insights into the CI phenomenon. With the understanding, we develop the destructive interference-based power adaptation (DIPA), an energy-efficient and distributed algorithm, that adapts transmission power to improve the performance of CI. Since CI-based protocols cannot have an explicit acknowledgment packet, we make use of *destructive* interference on a designated byte to provide a feedback. We leverage this feedback to adapt transmission powers. We compared CI with and without DIPA in two real-life testbeds. On one testbed, we achieve around 25% lower packet losses while using only half of its transmission power for 64-B packets. On the other testbed, we achieve 25% lower packet losses while consuming only 47% of its transmission power for 128-B packets. Existing CI-based protocols can easily incorporate DIPA into them to achieve lower packet losses and higher energy efficiencies.**

***Index Terms*— Concurrent transmissions, IEEE 802.15.4, constructive interference, wireless sensor networks, energy efficient communications, destructive interference.**

Manuscript received September 25, 2016; revised May 1, 2017 and February 1, 2018; accepted December 15, 2018; approved by IEEE/ACM TRANSACTIONS ON NETWORKING Editor K. Jamieson. Date of publication February 11, 2019; date of current version April 16, 2019. This work was supported in part by SCOTT through the Electronic Component Systems for European Leadership Joint Undertaking under Grant 737422 and in part by ZENLAB, IISc, Bengaluru, through the ANRC Project grants. This article was presented in part at the 35th IEEE INFOCOM 2016, San Francisco, CA, USA [1]. *(Corresponding author: Vijay S. Rao.)*

V. S. Rao and R. Venkatesha Prasad are with the Embedded and Networked Systems Group, Faculty of Electrical Engineering, Mathematics and Computer Science, Delft University of Technology, 2628 CD Delft, The Netherlands (e-mail: v.rao@tudelft.nl; r.r.venkateshaprasad@tudelft.nl).

T. V. Prabhakar is with the Department of Electronic System Engineering, Indian Institute of Science, Bengaluru 560012, India (e-mail: tvprabs@iisc.ac.in).

C. Sarkar is with TCS Research and Innovation, Kolkata 700160, India.

M. Koppal was with the Department of Electronic System Engineering, Indian Institute of Science, Bengaluru 560012, India. He is now with Continental AG, Bengaluru 560099, India

I. Niemegeers is with the Eindhoven University of Technology, 5612 AZ Eindhoven, The Netherlands.

Digital Object Identifier 10.1109/TNET.2019.2893597

I. INTRODUCTION

THE constructive interference (CI) phenomenon occurs when two or more nodes transmit the same data concurrently, which makes the signals superpose. Hence, receivers can decode the packet successfully with high probability due to, supposedly, the increased signal power at the receivers. Recently, Ferrari *et al.* [2] made a major contribution through their flooding technique called Glossy that exploits CI. Glossy achieves latency close to the lower theoretical limit and also implicitly synchronizes the nodes with sub-microsecond accuracy and with high reliability.

Several protocols that exploit CI have been proposed for data dissemination [2], [3] and data collection [4]. With the help of CI, these protocols eliminate the need for contention to access the wireless medium. Therefore, these protocols can achieve low latency and also be energy efficient. To achieve CI successfully with IEEE 802.15.4 radios operating in the 2.4 GHz band, the maximum tolerable temporal displacement between the concurrent transmissions is one chip duration, which is $0.5\,\mu$s. Ferrari *et al.* [2] achieve this tight bound with a radio-triggered synchronization mechanism and demonstrate this on Tmote Sky wireless sensor nodes.

Ferrari's work generated huge interest in the research community to study CI. However, from the previous studies, there appears to be an inconsistent and often contradicting picture about the working of CI. For example, while it is claimed in [2] that CI does not depend on the number of transmitters in the network, Noda *et al.* [5] report otherwise, namely, a significant decrease in packet reception when the number of transmitters increases. Another instance is that Ferrari *et al.* [2] claim that out-of-phase carrier waves from three or more concurrent transmitters do not hamper the decodability of the received signal although Wang *et al.* [6] derive a sufficiency condition for the phase of the concurrent signals such that they interfere constructively. This clearly demonstrates that we lack a complete picture of the CI phenomenon.

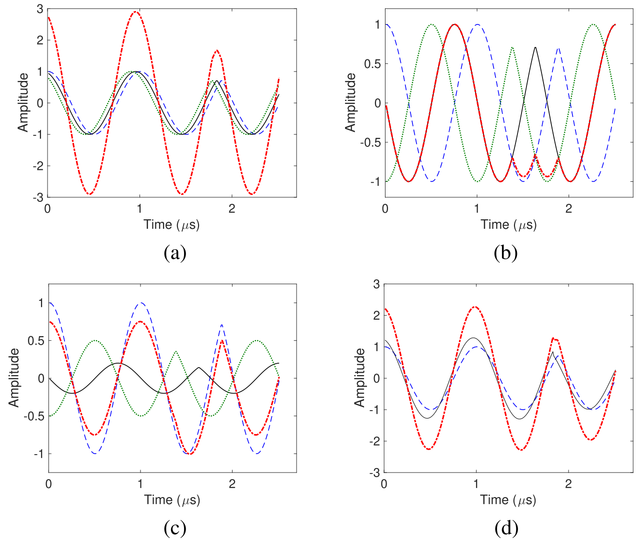

Fig. 1. The resultant signal (in red) when individual signals are aligned, have a temporal offset, have varying transmit powers and are subject clock errors on the radio. (a) Aligned signals. (b) Signals with a large phase offset. (c) Signals with different Tx power. (d) Signals from imperfect radio clock.

Several factors influence the performance of CI as commercial off-the-shelf IEEE 802.15.4 hardware is designed to work with a single carrier.

1) There is a high chance that the signals arrive with different phase offsets at the receiver for several reasons, including, distance between the transmitters and physical phenomena such as multipath, leading to failures in decoding the signals.
2) Furthermore, if nodes transmit with different powers, then the phase of the resultant signal is influenced by the strongest signal.
3) Clocks on the radio are allowed to have large drifts since compensating for drifts within one signal is easy. However, this can hamper CI.
4) Since sensor nodes are designed to be inexpensive, they have low accuracy crystals for the CPU clocks. Clock drifts can creep in to hinder CI.

Fig. 1 shows the resultant signal under the influence of some of these factors. Fig. 1(b) shows that the signal is not decodable when there is a large phase offset between the concurrent transmissions. However, the resultant signal can be decoded although the concurrent transmissions have a large phase offset when one signal overpowers the others as shown in Fig. 1(c). An example of signal from an imperfect radio clock is shown in Fig. 1(d).

The above aspects have not been studied holistically. This article aims to provide comprehensive insights into the impact of these factors with rigorous experimentation in different scenarios. Each scenario offers different radio propagation characteristics. We show that the performance of CI can be quite unreliable since it depends on several factors. Since protocols based on CI have been shown to be highly energy efficient coupled with very low latencies, the performance of CI should be improved. Based on the insights obtained from our experiments, we design Destructive Interference based Power Adaptation (DIPA), a transmit power adaptation based algorithm that improves the performance of CI. Protocols such as Glossy can benefit from DIPA to improve both performance, specifically bit error rates and packet losses, and save power on the nodes. This paper makes the following contributions:

1) We derive the resultant signal obtained from superposition of several concurrent transmissions in order to study CI from a receiver's perspective. Based on the resultant signal, we derive the maximum tolerable phase offset for achieving effective CI. Furthermore, we show the influence of various parameters from the expressions of the resultant signal.
2) We conduct for the first time an exhaustive experimental study of CI considering minute details in real-life settings. We validate the dependency on the factors through these experimental results.
3) One important result that we establish is that varying transmit powers can be beneficial to improve packet reception. Based on this, we propose DIPA, a localized algorithm that adapts transmit power based on feedback.
4) We propose to use *destructive* interference as a negative feedback mechanism for DIPA. We evaluate this algorithm on real-life sensor network testbeds. We show the improvement in the performance of CI due to DIPA as well as improvement in energy efficiency.

The paper is organized as follows. Sec. II summarizes the theory of constructive interference and the related work. We also list the claims and counter-claims made in the literature about the working of CI. Sec. III describes the experimental setup. In Sec. IV, we give expressions for the resultant signal and show through these equations, how CI depends on various parameters. We corroborate these with experimental results and draw our conclusions about CI also in Sec. IV. We establish that obtaining an optimal transmit power set has exponential complexity, and propose our algorithm with its evaluation in Sec. V. We make concluding remarks in Sec. VI.

II. Constructive Interference

In this section, we first summarize the theoretical background of constructive interference, and then briefly describe the literature that has studied CI and applications that use CI.

A. Theory of Constructive Interference

When two nodes transmit the same packet simultaneously on the same frequency band to a receiver within their transmission ranges, the transmitted signals superpose leading to *constructive* interference at the receiver. On an IEEE 802.15.4 node operating in the 2.4 GHz band, the data to be transmitted is first split into 4-bit groups each forming a symbol. Each symbol goes through a Direct Sequence Spread Spectrum (DSSS) modulation. Every symbol is modulated with a pseudo-random noise (PN) sequence of 32 chips. The symbol-to-chips mapping is defined in the IEEE 802.15.4 standard [7]. This baseband signal is then modulated onto the carrier with Offset-Quadrature Phase Shift Keying (O-QPSK), which is transmitted over the wireless medium.

At the receiver, a coherent detection method is used to demodulate the carrier signal. The signal is down-converted into chips, which are then mapped back to symbols. Redundancy introduced by the PN sequence allows for coping with errors caused on the channel. This redundancy improves the receiver sensitivity level at the cost of a reduced data rate.

For CI to occur, the tolerable temporal displacement between signals is $0.5\,\mu$s [2], since the chips in quadrature-phase (Q-phase) are delayed by the chip time, $T_c = 0.5\,\mu$s with respect to the in-phase (I-phase) carrier. As in [8], let the O-QPSK signal be represented by,

$$S(t) = I(t)\cos\omega_c t - Q(t)\sin\omega_c t. \tag{1}$$

Here, $I(t)$ is the I-phase, $Q(t)$ is the Q-phase component, and $\omega_c = \pi/2T_c$ is the radial frequency of half-sine pulse shaping. The resulting constructively interfered signal is given by,

$$S_r(t) = \sum_{i=1}^{K} A_i S_i(t-\tau_i) + N_i(t), \tag{2}$$

where, K is the number of concurrent transmitters, A_i is the amplitude and τ_i is the temporal offset of the i^{th} transmitted signal. $N_i(t)$ is the noise added to the signal.

B. Related Work

Energy-efficient data dissemination and collection protocols are the need of the hour with the proliferation of the Internet of Things [9]. We group the related work on CI into two categories: articles that study or analyze the CI phenomenon, and articles that use CI for protocol development in WSN.

Work on CI: With concurrent transmissions, a packet can be decoded by the receiver even in the absence of the capture effect. For concurrent transmissions to interfere constructively, precise timing requirements need to be imposed on the transmitter nodes. Ferrari *et al.* [2] analyze these requirements and outline a method to achieve them on CC2420 radios, specifically trying to make overall delay deterministic in nodes that have low accuracy clocks. Furthermore, they propose Glossy, a mechanism to flood the network within a few milliseconds. Importantly, they show through experiments on testbeds that (i) as the number of concurrent transmitters increases the packet reception ratio (PRR)[1] increases; (ii) the only factor that affects CI is not meeting the temporal offset constraint of $\leq 0.5\,\mu$s among concurrent transmissions.

Wang *et al.* [8] studied the scalability of CI. They argue that PRR of CI decreases with an increasing number of nodes due to non-deterministic delays. They show scalability is an issue, and propose an algorithm to handle it. The scalability issue has also been studied in [5], which demonstrates, with experiments, that more transmitters will affect the received signal severely.

A model for computing the success of packet reception under both CI and capture effect is proposed in [10]. Improving PRR in CI has been considered in [6] and [11]. Increasing the power difference among transmitters combined with the use of a forward error correction scheme is the method proposed in [11].

It is claimed in [6] that signals transmitted within $0.5\,\mu$s is not enough for CI due to the noise in the received signals. Further, they propose algorithms to achieve chip-level synchronization and select only those transmitters that improve the received signal power, with simplifying assumptions. From these studies, we make some observations.

Claim 1: Temporal offset among concurrent IEEE 802.15.4 transmitters not exceeding $0.5\,\mu$s will generate constructive interference with high probability [2].

Contradicting claim: Concurrent transmission with delay less than $0.5\,\mu$s is insufficient to guarantee CI due to noise in the radio signals [6].

Claim 2: Out-of-phase carrier waves allow correct detection with high probability, when the number of concurrent transmitters is greater than or equal to three [2].

Contradicting claim: Not all out-of-phase carriers allow the decoding of the packet correctly. A maximum tolerable phase offset to generate CI is derived in [6].

Claim 3: The number of concurrent transmitters have little impact on PRR [2].

Contradicting claim: CI does not scale with the number of transmitters due to the lack of coherence among carrier signals [5].

Claim 4: Non-deterministic delays are present and affect CI negatively [8].

Claim 5: Power imbalance greater than 5 dBm improves the PRR [5], where power imbalance is defined as two concurrent transmitters having transmission power levels that differ by a certain value. A similar claim is made in [11], in which power imbalance greater than 2 dBm improves the PRR.

Claim 6: PRR decreases when packets become longer [2].

It is apparent that there is an inconsistent view on the working of CI, and some claims are not completely explained and need substantiation. In this article, we shall establish how these parameters affect CI and perform experiments to validate them in various real-world scenarios.

Work on the use of CI: A node density estimation algorithm by counting the number of combined signals in CI based on the received power is proposed in [12]. The Splash protocol pipelines transmissions for parallel data dissemination over a tree using Glossy [3]. This work also demonstrates certain weaknesses of CI such as lower reliability of CI with larger packet sizes and that not all tightly synchronized transmissions are helpful. Splash uses several techniques, such as diversity in transmission density, opportunistic overhearing, channel cycling and XOR coding, to improve PRR. Ferrari *et al.* [4] propose a protocol utilizing Glossy to convert the multi-hop WSN to a shared, low-power wireless bus. This bus supports one-to-many, many-to-one and many-to-many traffic. Another work [13] modifies Glossy to make it a data collection protocol. While such protocols require all nodes to participate in concurrent transmissions, the authors of [14] propose a method to reduce them by selecting the nodes only in the direction of the destination. These protocols require reliable working of CI, which we investigate in this article.

III. Design of Experiments

We study the characteristics of CI both analytically as well as with experiments in real-life settings with twelve

[1]Packet reception ratio is the ratio of the number of data packets successfully delivered to the number of packets transmitted regardless of the number of transmissions involved in delivering each packet.

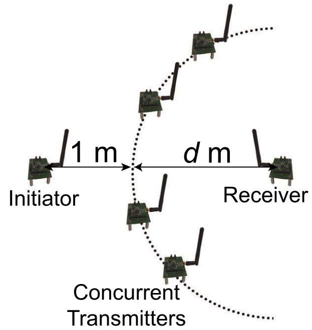

Fig. 2. Data collection setup in which concurrent transmitters are placed on an arc to make them equidistant from the receiver.

Fig. 3. Experimental setup in an empty office.

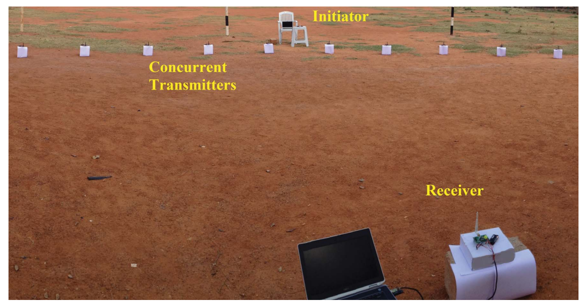

Fig. 4. Experimental setup in the field.

identical nodes. In this section, we describe the experimental setup used and the locations where experiments were conducted.

A. Experimental Setup

The setup is shown in Fig. 2. An initiator node is placed 1 m away from the set of relay nodes that also act as the concurrent transmitters. These nodes are placed on an arc, formed by the circle of radius d. A receiver is placed d m away, i.e., at the center of the circle, making receiver equidistant from the concurrent transmitters.

The distance between the receiver and the concurrent transmitters is chosen such that the network remains connected when any of the concurrent transmitters sends a packet at -6 dBm. That is, d is the threshold distance at which all the packets from a transmitter reaches the receiver successfully when transmitted with the specified power. Note that d varies across locations due to different radio propagation characteristics. In each location, we verified that connectivity exists and all packets were received between every (concurrent) transmitter node and the receiver.

We used the CC2530 system-on-chip solution from Texas Instruments [15], which supports IEEE 802.15.4 radio. CC2530 is controlled by an industry-standard 8051 microcontroller unit in the chip. The chip has a low-power consumption along with high receiver sensitivity (-97 dBm) and allows to choose transmit powers from -28 dBm to +4.5 dBm in 17 predefined steps. The radio also allows us to choose payload sizes from 1 B to 127 B. For our experiments, we used $\lambda/4$ antennas[2] with a reverse polarity SMA connector. We chose external antennas to eliminate any dependency of the performance of CI on the chip antennas. We implemented CI following the guidelines given in [2], and validated its proper working. That is, we ensured that the concurrent transmitters would transmit within a temporal offset less than 0.5 μs.

All nodes were powered by batteries that provided sufficient voltage levels throughout the experiments. We ensured that batteries had not caused any problems, by checking the voltage levels before and after the experiments to confirm that the measurements made were in good order.

[2]http://www.lsr.com/downloads/products/330-0016.pdf

Before each experiment, we ascertained that we used a channel in which there was no external interference from nearby WiFi or Bluetooth devices. No microwave appliances were nearby as well.

B. Locations

We conducted experiments at four different locations.

A model of an airliner fuselage: The fuselage is of dimensions 12 m $\times$ 3 m. The curved enclosure is made up of tin, and has wooden flooring. In this location, the radius of the arc, d, was 10.5 m.

Corridor: The corridor is 2 m wide and 27 m in length. Here, d was 23 m.

Office space: An empty office was another location for our experiments. It is 10 m $\times$ 7 m. In this location, d was 8 m. Fig. 3 shows the setup in the office space.

Soccer field: An outdoor location free from any construction was chosen. In this case, the radius of the arc was 8 m. Fig. 4 shows the setup in the field.

As mentioned before, each location offers different radio propagation characteristics. The signals reflect in the fuselage and the corridor locations, while the office space has less reflections since there are no obstacles. In the soccer field scenario, the signals are reflected only by the ground.

C. Data Collection Scenarios

All the experiments were conducted in a line-of-sight setting. We created seven scenarios for experimentation. At each

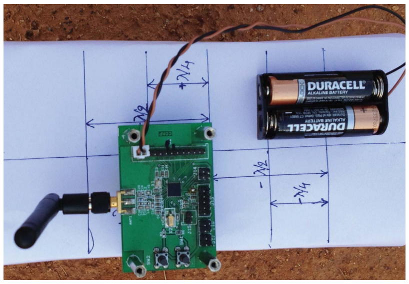

Fig. 5. Node movement for scenarios 6 and 7.

location, we collected data with at least 10,000 packets for various packet sizes in each scenario. Below is the list of scenarios.

Scenario 1: We started off with data collection with one transmitter and one receiver. At each step, we added one more transmitter. The transmission power of each concurrent transmitter was set to -6 dBm. This scenario studies the effect of the number of concurrent transmissions on a receiver.

Scenario 2: Scenarios 2–5 are created to study the effect of power imbalance among concurrent transmitters. In this scenario, alternate nodes were set to -6 dBm and -3 dBm.

Scenario 3: In this scenario, alternate nodes were set to transmission powers of -6 dBm and 1 dBm.

Scenario 4: In this scenario, every node chose a random transmission power between -10 dBm and +4.5 dBm.

Scenario 5: In this scenario, we considered 9 nodes out of which we created groups of three nodes. In each group, nodes transmitted at -6 dBm, -3 dBm and 1 dBm.

Scenario 6: In this scenario, 9 nodes were used. Alternate nodes were displaced by a distance of $\pm\lambda/2$ from the circumference of the circle, while the other nodes were on the circumference. Here, λ is the wavelength of the carrier wave. This scenario studies the effect of the distance between transmitters on the phase difference. The distance $\lambda/2$ was chosen since this would create a $180°$ phase offset between carrier signals of adjacent nodes.

Scenario 7: This scenario is similar to the previous scenario wherein the alternate nodes were displaced by $\pm\lambda/4$ instead of $\pm\lambda/2$. This scenario too studies the effect of the distance between transmitters on the phase difference as $\lambda/4$ separation would cause a $90°$ phase offset between carrier signals of adjacent nodes.

IV. Unfolding CI

In this section, we derive the amplitude and phase of the resultant signal. By phase, we refer to the phase of the carrier signal, unless mentioned otherwise. Based on these expressions, we analyze an exhaustive set of parameters on how they impact CI. Furthermore in this section, we corroborate this study with experimental results obtained from the setup and different scenarios described in the previous section. With these results, we present a holistic picture about CI.

A. Phase Offset

Carrier phase offset among the interfering signals can hinder constructive interference. Wang *et al.* [6] state that for CI to occur, the individual signals must also satisfy a sufficiency condition: for signals to interfere constructively, the phase offset of the i^{th} arriving signal should not exceed $|\phi_i| \leq \arccos\left(\sqrt{\frac{P_i}{P_S}}\right)/\omega_c$ from the strongest arriving signal with power P_S. Here, P_i is the power of the i^{th} signal. This implies that the maximum tolerable phase offset is $\pi/2$. While the condition seems intuitively correct since the I and Q components are offset by $\pi/2$, it is not completely realistic especially when the powers are different. We will show that even if P_i is only slightly less than P_S, but has a $\phi_i > \pi/2$, the signal can be decoded correctly.

To obtain the correct sufficiency condition, we take a more holistic approach to compute the phase, i.e., we derive the resultant signal and the tolerable phase offset.

Lemma 1: Constructive interference has occurred when the carrier phase offsets are within $\pm\pi/4$ with respect to each of the received signals at the receiver.

Proof: Eqn. (2) can be represented as $S_r(t) = \sum_{i=1}^{K} A_i \cos(\omega_c t + \phi_i)$, where ϕ_i is the phase of the i^{th} signal. For the sake of understanding the influence of the phase differences, we neglect noise from this equation. However, the negative influence from noise in phase detection and symbol recovery is an essential and basic element of the CI phenomenon, which is difficult to quantify.

From the Harmonic Addition theorem, the summation is given by,

$$S_r(t) = \sum_{i=1}^{K} A_i \cos(\omega_c t + \phi_i) = B\cos(\omega_c t + \hat{\phi}), \tag{3}$$

where,

$$B^2 = \sum_{i=1}^{K} A_i^2 + 2\sum_{i=1}^{K}\sum_{j>i}^{K} A_i A_j \cos(\phi_i - \phi_j), \tag{4}$$

$$\text{and } \hat{\phi} = \arctan\frac{\sum_{i=1}^{K} A_i \sin\phi_i}{\sum_{i=1}^{K} A_i \cos\phi_i}. \tag{5}$$

Here B is the amplitude of the resultant signal and $\hat{\phi}$ is the phase of the resultant carrier signal. This resultant signal is downconverted to baseband signal. There are two possible cases for this baseband signal.

Case 1: The signal is not decodable because the summation of several signals with different phase offsets produced a signal with invalid baseband phase information (see Fig. 1(b) for an example).

Case 2: The signal is decodable, i.e., CI has occurred. Even if the baseband phase offset of this decodable signal is greater than zero, the phase lock loop in the receiver attempts to correct the offset. This may be seen as the constellation being rotated by the baseband phase offset. Practically, this is possible for any phase offset if the preamble is sufficiently large.

In many implementations of O-QPSK based receivers (e.g., [16]), symbol recovery is done by taking hard decisions with respect to the axes of the constellation. In order to be correctly decodable, the symbols must be in the right quadrant to avoid detection errors. This is only possible if the baseband signal has a maximum phase offset of $\pm\pi/4$

with respect to the ideal constellation. This implies that this case is only possible if the phase offset of the resultant carrier, $\hat{\phi}$, is less than or equal to $\pm\pi/4$ with respect to each of the received signals at the receiver. Therefore, to decode correctly, the arriving signals are said to be interfering constructively when the maximum phase offset is $\hat{\phi} \leq \pm\pi/4$. ■

We now look at various sources that can alter the phase even if the temporal offset among transmitters is less than $0.5\,\mu$s.

1) Clock Errors and Number of Transmitters: There is a heavy reliance on the on-board clock to maintain synchronization. Typically, a crystal oscillator sources the clock for the microcontroller to execute instructions. In Tmote Sky nodes, a digitally controlled oscillator (DCO) acts as the source, which operates at a maximum of 8 MHz. However, this DCO is subject to errors of about $\pm 20\%$ from the nominal value, and temperature and voltage cause deviations of about $-0.38\%/°$C and $5\%/$V respectively [2].

Wang *et al.* [8] state that there can be uncertainty in time due to software delays, radio processing delays and clock drifts in each hop. Let p_e be the probability mass function (pmf) of the uncertainty of time delays on a node. With K concurrent transmitters, each being independent from the other transmitters, the effective pmf will be $p_e * p_e * \ldots K$ times $= p_e^K$. The probability that there are no clock drifts, i.e., no phase offsets with K concurrent transmitters decreases exponentially with increasing number of transmitters. The exponential curve represents the lower bound of success, i.e., occurrence of no clock drifts. Therefore, we can conclude that non-deterministic delays are present and can influence the resultant phase.

2) Distance Between Transmitters: The phase of the resultant signal is given by the following relation when two concurrent transmitters (assuming transmission powers are equal) are placed at distances d_1 and d_2 from the receiver respectively,

$$\phi = \frac{2\pi(d_1 - d_2)}{\lambda}, \tag{6}$$

where, λ is the wavelength. It is apparent that if these two transmitters are separated by a distance of $\lambda/2$, then they cancel each other. A generalization of this statement is that path differences between transmitters cause phase offsets, which in turn affects the resultant amplitude and hence, the decodability of the signal. For 2.4 GHz radios, the wavelength is $\approxeq 12.5$ cm. Hence, small path differences can create undesirable phase offsets.

3) Transmission Power: While clock drifts and distance can influence the phase of the resultant signal, intuitively, the signal with more power should dictate the amplitude and phase of the resultant signal. This is evident from Eqn. (4) and (5), i.e., when there is a stronger signal $S_i > S_j$, the value of B and $\hat{\phi}$ tends towards the value of A_i and ϕ_i. We demonstrate this with the following example. We consider two concurrent transmitters. We fix the amplitude and phase of one signal to constant values, namely $A_1 = 1V$ and $\phi_1 = \pi/4$. We fix only the phase of the second signal at $\phi_2 = 5\pi/6$ and vary only the amplitude from 0.00 V to 2.00 V in steps of 0.01 V. Fig. 6 shows the amplitude and phase of the resultant signal computed from Eqn. (4) and (5). There is a point of discontinuity in the phase at a certain point, and it begins tending towards the second signal, as it gets stronger. In the example in Fig. 6, when the powers of the two signals vary, the resulting signal can be correctly decoded although A_2 has a phase offset greater than $|\phi_2| > \pi/2$. For the example in Fig. 6, we computed the regions in which the resultant signal can be decoded as either S_1 or S_2. The resultant signal is taken to be decoded when it has a correlation coefficient greater than or equal to 0.99 of the decoded signal with either S_1 or S_2. The region between these two points do not correspond to either of the transmitted signals and cannot be decoded. However, we have demonstrated that concurrent transmissions with varying powers and phases can still be decoded, which is in contradiction with the sufficiency condition from Wang *et al.* [6].

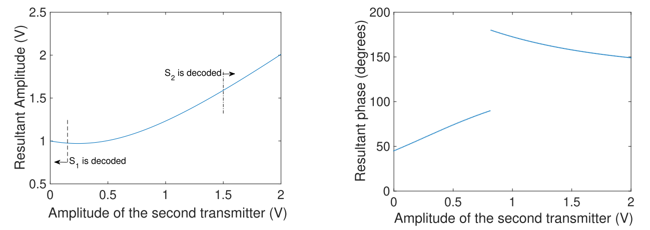

(a) (b)

Fig. 6. (a) Resultant amplitude and (b) phase when $A_1 = 1$ V and $\phi_1 = \pi/4$. Amplitude A_2 is varied from 0 to 2 V in steps of 0.01 V and its phase is $\phi_2 = 5\pi/6$.

4) Physical Environment: Another factor that affects the phase of the resultant signal is the physical environment where the sensor nodes are deployed. Multipath is unavoidable in many real-world deployments. Due to this effect, concurrently transmitted signals travel different path lengths. Therefore, the receiver will see different phase offsets of the signals. Although several channel models exist, it is difficult to quantify the exact influence of multipath signals on the received signal. Nevertheless, it should not be neglected and can clearly be seen in an actual deployment. We shall demonstrate this in the following section.

Lemma 2: A packet can be decoded with high probability when concurrent transmissions of the same packet have (a) the temporal offset between transmissions $\leq 0.5\,\mu$s; (b) the phase offset of the resultant signal $\leq \pm\pi/4$ with respect to each other for the received signals; (c) different transmission powers for the individual transmissions.

Proof: Conditions (a) and (b) are the necessary and sufficiency conditions for constructive interference. Condition (a) has been proven in [2] and condition (b) has been proven in Lemma 1. The necessary and sufficiency conditions hold when the transmission powers employed by the concurrent transmitter are equal. Condition (c) specifies the special case when either (a) or (b), or both are not met. With Lemma 1 and the discussions thereafter, it is clear that when transmission powers of the individual concurrent transmissions are different, the phase offset is determined by the stronger arriving signal and has higher chances of being decoded. When the transmission powers of the individual signals vary with time offsets of transmissions close to $0.5\,\mu$s, which is much lower than the preamble time, there is a non-negligible chance of (power) capture taking place [17], i.e., the ability of the radio to receive

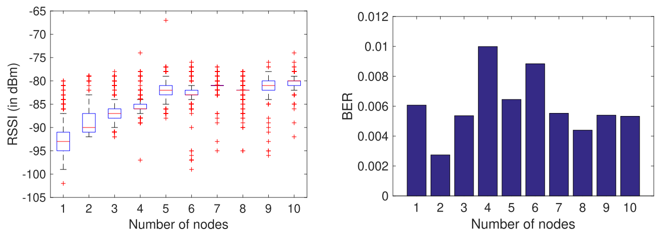

(a) (b)

Fig. 7. (a) RSSI and (b) BER values in an empty office with receiver at 8 m from concurrent transmitters.

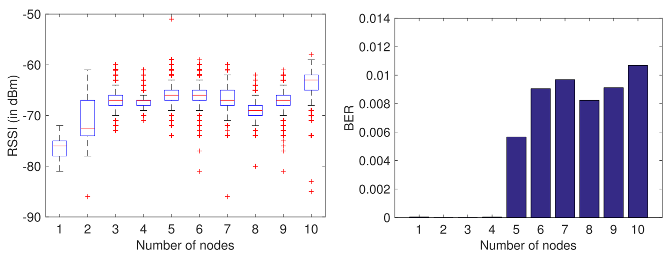

(a) (b)

Fig. 8. (a) RSSI and (b) BER values in an empty office with receiver at 1 m from concurrent transmitters.

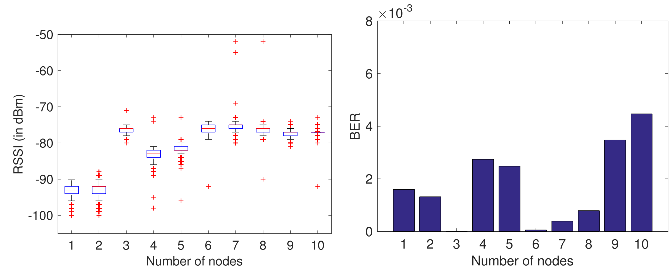

(a) (b)

Fig. 9. (a) RSSI and (b) BER values in a model airliner fuselage with receiver at 10.5 m from concurrent transmitters.

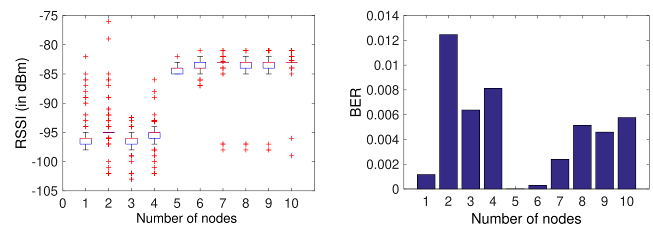

(a) (b)

Fig. 10. Multipath effects in corridor. (a) RSSI. (b) BER.

a strong signal regardless of other concurrent transmissions. When the tight time synchronization of $0.5\,\mu$s cannot be met due to synchronization errors or clock drifts, there is still a high probability of the packet being decoded correctly. ■

The significance of Lemma 2 is as follows: concurrent transmissions increase the probability of packet reception either through constructive interference or capture effect (when different transmission powers are employed). While condition (c) is not what we aim for, in practice, it is difficult to know whether CI or capture occurred at the receiver for a successful packet reception, which will be discussed in the following section. However, it is difficult to quantify the probability of correct reception analytically due to noise and other various parameters affecting the signal.

5) Observations: Since we are investigating the phenomenon of CI over one hop, we look at statistics of each transmitted packet rather than the PRR.

Here, we are interested in received signal strength (RSSI), bit error rate (BER) and packet loss. For brevity, we present selected data from different scenarios to best describe the effect of parameters on CI. The inferences drawn here are applicable to data from all scenarios since the trends were similar. While some conclusions can be derived from previous work, we present them here for the sake of completion. Together with our inferences, this work provides comprehensive insights into CI.

Fig. 7 shows the RSSI and BER values at the receiver in the empty office scenario. The RSSI increases with increasing number of concurrent transmitters before saturating at a certain power. However, when we look at the BER, we see that BER does not follow the nice trends as the RSSI; nor does a high RSSI imply less errors. We also placed an additional receiver in this scenario at 1 m distance from the concurrent transmitters. The RSSI and BER values at this receiver (see Fig. 8) also depict the same trends. Fig. 9 shows the RSSI and BER in the fuselage location when the nodes are kept at 10.5 m distance. In this case, we observe that the RSSI does not follow the nicely increasing trends especially with 4 and 5 concurrent transmitters. We speculate that the some signals were not contributing to the decoded signal and hence lower RSSI. BER, in this experiment too, does not show any relation with RSSI. The causes for lower BER could be due to one or more factors influencing the phase of the resultant, such as clock errors, number of transmitters, and the physical environment, as discussed in the previous section. From this figure, we infer the following:

Inference 1: CI increases the energy in the wireless channel.

Inference 2: Higher RSSI does not imply lower BER of the packet.

Inference 3: Temporal offset $\leq 0.5\,\mu$s is necessary for CI to occur with high probability. However, achieving this tight synchrony is not always sufficient to reap the maximum benefits of CI.

Inference 4: There is no relationship between BER and the number of nodes, i.e., we cannot conclude that the number of concurrent transmitters will influence the PRR.

Although we achieved a tight synchronization of $0.5\,\mu$s on the nodes, we saw that the BER shows variation in performance. This leads us to the third inference. The sufficiency condition in Lemma 1 was probably not satisfied here. We will now illustrate the fourth inference better with another dataset.

Fig. 10 shows the RSSI and BER for varying number of transmitters in the corridor environment. We strongly suspect that multipath is influencing the received signals. In a corridor with one transmitter, multipath will mostly be beneficial as the corridor will act as a waveguide (also evident from Fig. 10(b) and 7(b)). However, in order to realize CI, both the conditions for the temporal and phase offsets as stated in Lemma 1 must be satisfied. Although the concurrent transmitters may be well synchronized, the path lengths traversed by the individual transmissions may be different. This leads to a new problem that arises with concurrent transmissions.

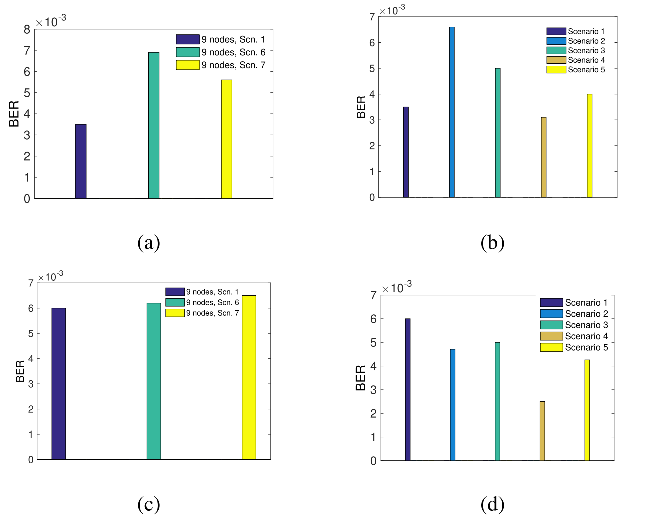

Fig. 11. BER in various scenarios in two different locations. (a) BER in the fuselage with node displacement. (b) BER in the fuselage with 9 concurrent transmitters in various scenarios. (c) BER in the soccer field with node displacement. (d) BER in various scenarios with 9 concurrent transmitters in the soccer field.

The influence of multipath with concurrent transmitters can be seen in Fig. 10(b), which shows that multipath can significantly impact the BER. It seems that the signal from the fifth node is more 'influential' since the RSSI suddenly steps up after the fifth node is added and BER reduces as well. Note that all nodes used the same transmit power. The fifth node was the third node from either side of the walls, in different experiment trials, much closer to the walls than nodes 1 to 4. We can therefore infer the following:

Inference 5: There is a definite influence of the set of transmitters on CI that are participating in concurrent transmissions.

Inference 6: The phase of the resultant signal is influenced by multipath.

Inference 5 is easily observable in Fig. 10(b), wherein adding the fifth node performed better than even with a single transmitter. When signals are bounced off, they take varied path lengths, which is one of reasons for Inference 6. This inference is also in line with the discussions in the previous section. We will illustrate it with another experiment.

Fig. 11(a) and Fig. 11(c) show the BER for different scenarios when the nodes are displaced by $\lambda/2$ (Scenario 6) and $\lambda/4$ (Scenario 7) in the fuselage and the soccer field respectively. Here it is apparent that the change in path length has increased the bit errors.

Inference 7: The phase of the resultant signal is influenced by the distance between concurrent transmitters.

The last study is about the transmit power difference among transmitters. For this study, we pick the data from the fuselage and the soccer field scenario with a payload of 127 B (worst BER case). We see the BER from various scenarios in Fig. 11(b) and Fig. 11(d) for the fuselage and the field respectively. It is clear that different transmit powers have a positive effect on CI, as described in Sec. IV-A. Across experiments, it was difficult to infer whether 3 dBm or 7 dBm difference in transmit power performed better. Fig. 11(b) shows an exception when different transmit powers increase the errors. But in all cases, when the transmit powers were randomly chosen (Scenario 4), the obtained BER was the least. Clearly, a power imbalance is effective, but it is difficult to find a common threshold of the imbalance that improves the performance of CI.

Inference 8: Transmitting at higher power usually results in better packet reception. However, power imbalance among concurrent transmitters can also aid packet reception.

There are two reasons for this observation (see Lemma 2): (a) as stated in Sec. IV-A, the stronger signal dictates the resultant signal amplitude and phase offset; (b) capture effect could occur. One interesting question that arises here is when does the *power* capture occur in this concurrent transmissions. Son *et al.* [18] empirically claim a 6 dBm difference as the threshold, however, the payloads were different from each transmitter. Recently, Wilhelm *et al.* [19] conducted extensive work on capture effect by using a simulator that is accurate at symbol-level. When the payloads were the same, it was quite difficult for them too to indicate what part of successful reception was due to capture effect.

B. Clock Drifts on the Radio and Packet Size

It is well-known that the bit error rate increases with increasing packet size. In the case of a single transmitter, this observation is attributed to the error-prone wireless channel. However, with CI, there is another factor that causes the increase in bit error rates with increasing packet size even if the channel is coherent throughout the transmission.

Apart from the clock for the microcontroller, there is another oscillator in the radio module. IEEE 802.15.4 specifies that the radio can tolerate up to $\pm$40 ppm clock drifts [7] when receiving the carrier signal. That is, the total frequency offset between two concurrent transmitters can be up to 80 ppm. This causes the signals to be distorted (an example is shown in Fig. 1(d)). While an automatic frequency control unit can be employed for compensating the frequency offset, this is not employed due to the additional circuitry and cost factors. This offset is fine when receiving a single carrier signal since it can be recovered easily at the cost of decreased sensitivity level. However, with CI given that the signals have non-zero phase offsets, the frequency offsets start impeding the signal and the bits are decoded in error [10].

Fig. 12 shows the BER for different packet sizes from the experiments in the soccer field. As expected, longer packet sizes are prone to error. To illustrate the clock errors on the radio, we plot the bit error rate per bit position in a payload of 127 B (1016 bits) in Fig. 13. We see huge variations in errors for 3 nodes and the trend of errors seems to increase with subsequent bit positions. To capture this trend, we fit a line to the data which is shown in bottom plot of Fig. 13. The slope is increasing in both the cases of two and three nodes but seems negligible for the two node case, while it is clear the errors are increasing with three nodes.

Inference 9: Bigger packet sizes are prone to more errors due to both the wireless channel and higher carrier frequency offset caused by low accuracy clocks in the radio.

Inference 10: The number of concurrent transmitters will influence the BER for bigger packet sizes due to erroneous clocks on the radio.

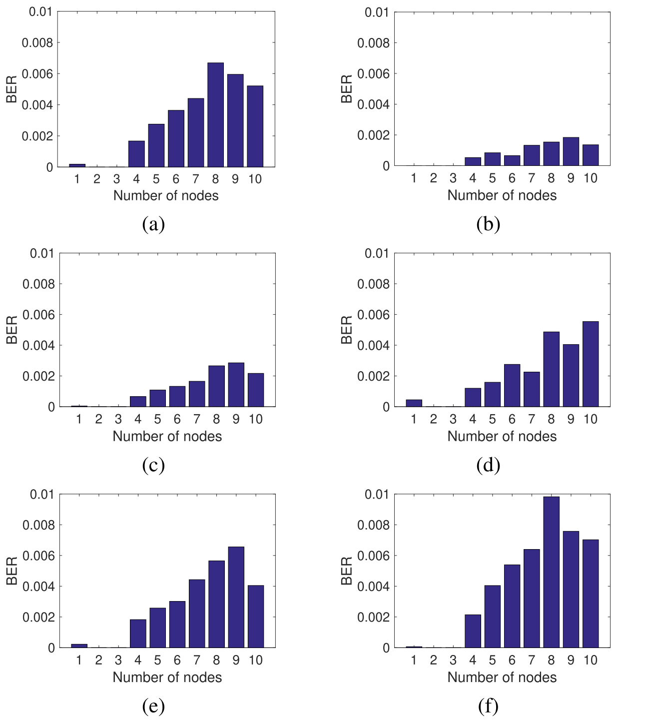

Fig. 12. BER in the soccer field for different packet sizes. (a) Average of all packet sizes. (b) Packet size 16 B. (c) Packet size 32 B. (d) Packet size 64 B. (e) Packet size 96 B. (f) Packet size 128 B.

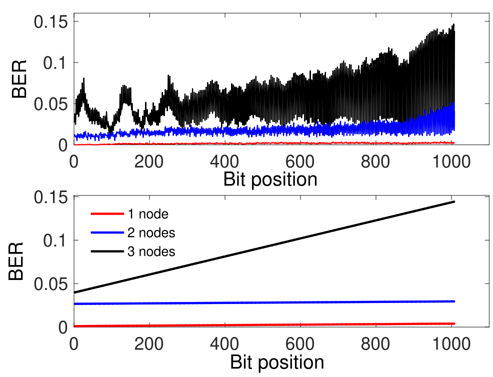

Fig. 13. Top: BER per position for a 127 B payload with varying number of concurrent transmitters. Bottom: Linear fitting to show the slope of BER at different bit positions.

V. Improving the Performance of CI With DIPA

Many works such as the ones mentioned in Sec. II-B employ CI over multihop wireless sensor networks. For example, Low-power wireless bus [4] builds a collection and dissemination protocol over Glossy that is demonstrated to be highly energy-efficient as compared to other similar protocols. These works, including Glossy, transmit the packets more than once to ensure reliable packet delivery. Since CI can have a bad performance, it is important to improve the performance of CI that also increases the energy-efficiency without impeding the benefits of CI.

As demonstrated in the previous section, minimum BER from CI can be obtained only when all the parameters are just *right*, which is almost impossible due to many associated practical difficulties. Furthermore, in a random deployment, which is typical of a WSN, each receiving node may see a different BER. Nevertheless, there are two methods to improve CI: (a) reducing non-deterministic delays on the nodes; (b) choosing the transmission powers for each node that maximize CI. There has been considerable work to improve the performance of CI by reducing non-deterministic delays [6], [8]. However, while synchronization is necessary, the performance is still limited by the deployment as we have seen in the previous sections. To this end, setting transmission powers for each node is more beneficial (see Inference 8).

The problem of choosing the set of transmission powers for all concurrent transmitters that maximize CI, while achieving energy efficiency, in the network has an exponential number of combinations. Energy efficiency is important since the nodes are battery-powered. Let each node have Γ transmission power levels to choose from. With K concurrent transmitters, in the worst case number of combinations that need to be evaluated are of the order $O(\Gamma^K)$. Furthermore, given that the wireless channel changes over time, a static set of transmission powers will not help in the lifetime of the network. A limitation of a real-life deployment with Glossy or other CI based protocols is that there are no ACK packets; nor can ACK packets be introduced since the transmissions are not unicast.

Under these conditions, we propose an algorithm Destructive Interference based Power Adaptation (*DIPA*) that adapts transmission power based on the performance of CI. The performance is obtained through *feedback*. To this end, we utilize *destructive interference* (DI) to gather feedback from the neighboring nodes. We first describe how DI works, before describing the algorithm.

A. Destructive Interference of Symbols

Given that CI achieves tight synchronization at chip level, we can achieve DI at a symbol level. At the receiver, if many dissimilar symbols overlap then symbol recovered can be any symbol from the set of all symbols. However, if two dissimilar symbols overlap at the receiver, then the decoded symbol is probably going to be either of them. For example, if symbols 0x0 (or $\mathtt{S}_0$) and 0x1 (or $\mathtt{S}_1$) are transmitted, the receiver demodulates and uses a soft-decoding procedure to get the chip sequence. This sequence may not correspond to any of the symbols. A hard-decision procedure follows to map the decoded sequence to one of the symbols, wherein symbol with the highest correlation to the decoded sequence is used as the decoded symbol. In this case, the "distance" from 0x0 is lower than that of 0x1.

We simulate DI between all combinations of symbols taking two at a time in MATLAB and derive the decoded symbol as shown in Fig. 14. When we look at the upper triangular matrix of this symmetric matrix, we observe that symbol $\mathtt{S}_0$ is the most likely symbol to be decoded when it interferes with any other symbol (except in five cases). In general, the first eight symbols are more *robust* than the last eight symbols [20]. The last symbol, $\mathtt{S}_{15}$ is the least likely symbol to be itself.

In order to exploit this as a feedback mechanism, we make use of the above observation: we select $\mathtt{S}_{15}$ to represent ACK. When nodes have to send NACK, they send $\mathtt{S}_0$. We take

Symbol 2 \ Symbol 1	S_0	S_1	S_2	S_3	S_4	S_5	S_6	S_7	S_8	S_9	S_{10}	S_{11}	S_{12}	S_{13}	S_{14}	S_{15}
S_0	0	0	0	3	0	0	6	7	0	0	0	0	12	13	0	0
S_1	0	1	1	1	4	0	1	7	1	1	1	1	1	13	14	1
S_2	0	1	2	2	2	5	1	2	2	2	2	2	2	2	14	15
S_3	3	1	2	3	3	3	6	2	8	3	3	3	3	3	3	15
S_4	0	4	2	3	4	4	4	7	8	9	4	4	4	4	4	4
S_5	0	0	5	3	4	5	5	5	0	9	10	5	5	5	5	5
S_6	6	1	1	6	4	5	6	6	6	1	10	11	6	6	6	6
S_7	7	7	2	2	7	5	6	7	7	7	2	11	12	7	7	7
S_8	0	1	2	8	8	0	6	7	8	8	10	1	8	6	8	8
S_9	0	1	2	3	9	9	1	7	8	9	9	11	2	9	7	9
S_{10}	0	1	2	3	4	10	10	2	10	9	10	10	12	3	10	0
S_{11}	0	1	2	3	4	5	11	11	1	11	10	11	11	13	4	11
S_{12}	12	1	2	3	4	5	6	12	8	2	12	11	12	12	14	5
S_{13}	13	13	2	3	4	5	6	7	6	9	3	13	12	13	13	15
S_{14}	0	14	14	3	4	5	6	7	8	7	10	4	14	13	14	14
S_{15}	0	1	15	15	4	5	6	7	8	9	0	11	5	15	14	15

Fig. 14. Decoded symbol after destructive interference for different combination of symbols from two concurrent transmitters. The number in each cell indicates the decoded symbol.

a conservative approach here, i.e., the symbol representing ACK is the symbol that is least likely to be itself when it overlaps with another symbol. In contrast, the NACK is the most robust symbol, i.e., S_0. There can be multiple concurrent transmitters sending either of these two symbols. The feedback symbols experience the same phenomena as CI, therefore the decoded symbol depends on several parameters such as number of transmitters, clocks, multipath, transmission powers and capture effect. In order to be even more conservative, at the receiver, if the feedback is any symbol other than S_{15}, then it is considered to be NACK. Thus, DI allows us to capture the feedback of the channel and other errors well.

With the feedback mechanism in place, we first describe the algorithm for a single hop case, and then show how to integrate it into Glossy for more practical applications.

B. DIPA Algorithm

We designed the DIPA algorithm considering a random deployment of nodes, wherein each receiving next hop node can experience a different BER and packet reception with the same set of concurrent transmitters. The intuition behind the algorithm is simple: increase transmit power if packets are not being received successfully, and slowly decrease the power if the packet reception is stable. The idea is to make transmissions as reliable as possible while conserving energy.

One byte (i.e., we choose two symbols since we lose only four bits) is used as feedback and is appended to the data. Each concurrent transmitter takes this decision locally and independently, based on the feedback it receives from the neighboring nodes. Note that each concurrent transmitter might also see a different feedback due to the same effects as on CI and the probability of correct detection. A caveat to the working of this mechanism is that the CRC of the packet should be computed in software except for the feedback. At the receiver, the CRC should be checked except for the feedback. This software based CRC computation is allowed in most radios [15].

To explain the algorithm, we consider a one-hop setup similar to Fig. 2. The algorithm is equally applicable when the concurrent transmitters are randomly placed, and when there is more than one receiver. Here, the source sends a packet, which is forwarded by the concurrent transmitters to the receivers. The receivers validate the packet reception by checking its CRC. ACK is sent if the packet is received correctly, otherwise a NACK is sent. If no packet is received, i.e., even with an invalid CRC due to noise or insufficient transmit power, then a timeout occurs on the concurrent transmitters. In this case, a NACK is sent in the subsequent packet that is to be forwarded. The algorithm for adapting the power based on feedback on a concurrent transmitter is given in Alg. 1. The function OnReceiveTimeOut is called when ACK packet is not received, which can occur when: (a) the packet sent not received by any receiver; (b) the packet sent was received but could not pass the CRC check or (c) the receiver's transmission power is too low to be received correctly. The function OnReceive is called when a packet is received. This implies that at least one receiver was able to decode the sent packet correctly. As mentioned earlier, different transmission powers of the concurrent transmissions set by DIPA can impact negatively for CI. A negative feedback implies that earlier sent packets were not being received correctly, therefore, transmit power is increased for the subsequent packets. Nodes decrease their transmit power only when they observe G_{TH} consecutive successful reception. If transmission fails or time out occurs, the transmit power is increased. When the maximum transmit power fails to get ACKs, then the nodes resort to a random power level, hoping for the best.

In a multihop case where Glossy is used, every node receiving a packet will re-broadcast it a predefined number of times. To use DIPA here, we simply append the feedback into the Glossy payload. The only change is in the notion of ACK in Alg. 1, i.e., the concurrent transmitters wait for actual data packets instead of ACK packets from the neighboring nodes.

The worst case running time of DIPA is O(1). While DIPA should not cause any timing issues, however in case there arises such an issue, then the feedback can be collected for every packet but power adaptation can be executed after every few packets to suit the needs of the protocol.

C. Evaluation

We used an implementation of Low-power Wireless Bus [21] in Contiki, which bases its working on Glossy, for our evaluation purposes. Although original Glossy transmits each packet at least twice to guarantee a high PRR, we modify this aspect of Glossy to make only one transmission of each packet since we are interested to evaluate the performance of CI. We also implemented DIPA into this Glossy implementation for evaluation purposes.[3] We set G_{TH} to 5, and use {-5 dBm, -3 dBm, -1 dBm, 0 dBm} as the set of transmission powers on the nodes. We compare the performance of CI in Glossy and DIPA with respect to BER, packets loss ratio and the

[3]Our implementation is available at https://github.com/vijaysrao/dipa

Algorithm 1: DIPA Algorithm on a Concurrent Transmitter

// Let p_s be the next packet to be sent, and p_r be the packet that is received
Initialize $nSuccess \leftarrow 0$
function OnReceiveTimeOut
  $nSuccess \leftarrow 0$
  if *GetTxPower*() == MAX_TX_POWER
    ChooseRandomTxPower()
  else
    IncreaseTxPower()
  end if
  p_s.*SetFeedback*(NACK)
end function
function OnReceive Packet p_r
  if p_r.*IsCRCValid*() == FALSE **then** // Incorrect Tx power from the receiver
    p_s.*SetFeedback*(NACK)
  else
    $nSuccess \leftarrow nSuccess + 1$
    p_s.*SetFeedback*(ACK)
    if p_r.*GetFeedback*() == NACK // Previous packets were not being received
      if *GetTxPower*() == MAX_TX_POWER
      else
        ChooseRandomTxPower()
      end if
      IncreaseTxPower()
    else
      Everything is just fine
      if $nSuccess \geq G_{TH}$
        DecreaseTxPower() $nSuccess \leftarrow 0$
      end if
    end if
  end if
end function

transmission powers used, for different packet sizes. Packet loss is said to occur when a transmitted packet fails to reach the receiver or when the CRC check on the received packet is reported as failure.

We evaluate our algorithm in two real-life testbeds w-ilab.t [22] and Indriya [23]. We used 45 nodes on the third floor of the w-ilab.t office testbed, and 37 nodes on the first floor of the Indriya testbed. Both the testbeds contain devices with CC2420 radio. The nodes are randomly deployed in both testbeds, and have a mixture of both line-of-sight and non line-of-sight links. We choose the testbeds since such a scenario is more common in real-life deployments.

We first present results from w.iLab.t testbed. In this testbed, we compare DIPA with Glossy transmitting at two different powers. All values are averaged over the data from all the nodes and experiments, and are normalized with respect to Glossy with high transmission powers (Glossy (HP)). Glossy (LP) represents the case where the nodes employ lower

TABLE I
TRANSMIT POWERS IN W.ILAB.T TESTBED

Algorithm	Tx Power Consumed (in %)
Glossy (HP)	100
Glossy (LP)	40
DIPA (16B)	52
DIPA (32B)	58
DIPA (64B)	60

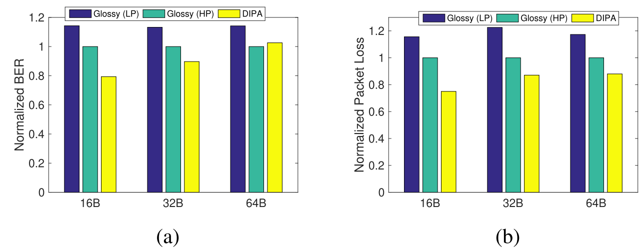

Fig. 15. Comparison between Glossy and Glossy with DIPA in w.iLab.t testbed. (a) Normalized BER. (b) Normalized packet loss.

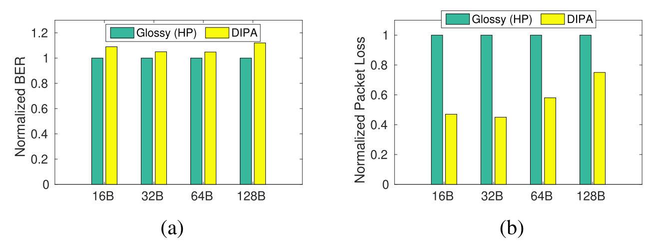

Fig. 16. Comparison between Glossy and Glossy with DIPA in Indriya testbed. (a) Normalized BER. (b) Normalized packet loss.

TABLE II
TRANSMIT POWERS IN INDRIYA TESTBED

Algorithm	Tx Power Consumed (in %)
Glossy (HP)	100
DIPA (16B)	36
DIPA (32B)	38
DIPA (64B)	40
DIPA (128B)	47

transmission power. We consolidate results in Table I and Fig. 15.

Glossy trades off energy for better BER and packet reception, which is evident from Fig. 15 when compared between Glossy (LP) and Glossy (HP). DIPA adapts power based on the feedback in order to achieve lower packet losses than Glossy. This can be seen from the table and the figures that our method performs as good as Glossy with respect to BER, reduces packet losses and consumes lower power than Glossy for a better performance. Compared to Glossy with 16B packets, DIPA achieves better BER with 25% lower packet loss and around 48% savings in transmission powers. Similarly, for 32B packets, DIPA achieves a better BER with 10.5% lower packet losses and 42% of power savings. While BER increased negligibly with 64B packets, we used 40% lower power to achieve 12% lower packet losses.

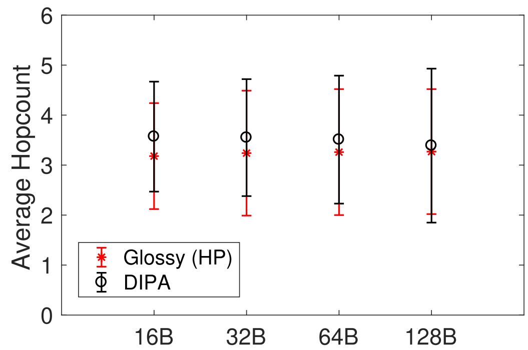

Fig. 17. Average and standard deviation of hopcounts for various payload sizes using Glossy (HP) and DIPA on the Indriya testbed.

Based on the above results, we set Glossy (HP) as the benchmark and only compare DIPA against it in the Indriya testbed. We see in Fig. 16(a) that DIPA results in higher BER than Glossy (HP). However, the higher BER does not result in higher packet losses. In fact, the packet losses with DIPA are much lower than Glossy (HP) for all packet sizes as can be seen in Fig. 16(b). This is because packets experienced bursty errors with DIPA. When concurrent transmitters send with different transmission powers that result in a decodable packet, the packet has no or minimum errors due to the influence of one or more high power signals. However, when the packet is undecodable, the packet contains many bit errors. This leads to the bursty errors.

Compared to DIPA, Glossy achieves better BER between 5-12% over different packet sizes. However, DIPA outperforms Glossy with only 53%, 54%, 42% and 25% lower packet loss for 16 B, 32 B, 64 B and 128 B packets. The savings in transmission powers can be computed from Table II.

Fig. 17 shows the average and standard deviation of the hop counts obtained for various payload sizes using Glossy (HP) and DIPA on the Indriya testbed. We observe that when DIPA consumes less transmission power the average number of hops increases, but only slightly. The reason for only the slight increase is that if one of the concurrent transmitters transmits at a higher transmission power, then the hop count is reduced. Furthermore, since the payload size directly affects the number of errors, DIPA utilizes more transmission power to circumvent this. Thus, transmission power increases in DIPA (see Table II). Therefore, we observe that the average hop count decreases as payload size increases for DIPA.

The number of hops can change per packet in DIPA as it switches the transmit powers on the nodes depending on the feedback. In the case when the number of hops increases, some concurrent transmitters may waste energy on idle-listening for a data packet that arrives at a later time due to the changed scenario. We observe from Fig. 17 that the number of hops do not vary significantly (due to the chosen set of transmit powers), which implies this energy wastage is not significant. As Glossy resynchronizes periodically, the nodes can adjust their wakeup times leading to a reduction in energy wastage. Such energy expenditure can be minimized by choosing a set of transmit powers that do not significantly change hop counts in DIPA, and by increasing G_{TH} (prevents rapid switching to lower transmit powers).

VI. Conclusions

Constructive Interference (CI), due to its simplicity, has redefined services and applications, and opened up new avenues in wireless sensor networks. Various studies, hitherto, on CI portrayed an inconsistent view of its working, limitations and benefits. In this paper, we extensively studied CI from the point of view of receivers both analytically and experimentally. Specifically, we derived the expressions for resultant signal and listed the parameters that affect CI. We established how these parameters influence performance of CI and validated our arguments with results from exhaustive experiments considering minute details, such as half wavelength distance differences among the transmitters, power, etc. Finally, we drew inferences on the working of CI in real-life settings capturing various situations. We believe that our work is one of the first to provide a holistic view of CI and its effects in various scenarios. While the experiments were conducted for line-of-sight scenario, they are applicable to other settings too.

Further, we proposed *DIPA*, a distributed algorithm that is energy-efficient. It improves packet reception by adapting transmission powers, and enhances reception due to power capture. This algorithm leverages destructive interference to gain feedback about packet reception with CI. We evaluated our algorithm on a real-life testbed against Glossy, and showed significant energy savings and better packet reception in real-life testbeds.

References

[1] V. S. Rao, M. Koppal, R. V. Prasad, T. V. Prabhakar, C. Sarkar, and I. Niemegeers, "Murphy loves CI: Unfolding and improving constructive interference in WSNs," in *Proc. IEEE 35th Annu. Int. Conf. Comput. Commun. (INFOCOM)*, San Francisco, CA, USA, Apr. 2016, pp. 1–9.

[2] F. Ferrari, M. Zimmerling, L. Thiele, and O. Saukh, "Efficient network flooding and time synchronization with glossy," in *Proc. 10th ACM/IEEE Int. Conf. Inf. Process. Sensor Netw. (IPSN)*, Apr. 2011, pp. 73–84.

[3] M. Doddavenkatappa, M. C. Chan, and B. Leong, "Splash: Fast data dissemination with constructive interference in wireless sensor networks," in *Proc. NSDI*, 2013, pp. 269–282.

[4] F. Ferrari, M. Zimmerling, L. Mottola, and L. Thiele, "Low-power wireless bus," in *Proc. 10th ACM Conf. Embedded Netw. Sensor Syst.*, 2012, pp. 1–14.

[5] C. NodaCarlos, M. Pérez-Penichet, B. Seeber, M. Zennaro, M. Alves, and A. Moreira, "On the scalability of constructive interference in low-power wireless networks," in *Proc. 12th Eur. Conf. Wireless Sensor Netw.*, 2015, pp. 250–257.

[6] Y. Wang, Y. He, D. Cheng, Y. Liu, and X.-Y. Li, "Triggercast: Enabling wireless constructive collisions," in *Proc. INFOCOM*, Apr. 2013, pp. 480–484.

[7] *IEEE Standard for Low-Rate Wireless Networks*, IEEE Standard 802.15.4-2015, 2011.

[8] Y. Wang, Y. He, X. Mao, Y. Liu, and X. Y. Li, "Exploiting constructive interference for scalable flooding in wireless networks," *IEEE/ACM Trans. Netw.*, vol. 21, no. 6, pp. 1880–1889, Dec. 2013.

[9] M. Zheng, L. Chen, W. Liang, H. Yu, and J. Wu, "Energy-efficiency maximization for cooperative spectrum sensing in cognitive sensor networks," *IEEE Trans. Green Commun. Netw.*, vol. 1, no. 1, pp. 29–39, Mar. 2017.

[10] D. Yuan and M. Hollick, "Let's talk together: Understanding concurrent transmission in wireless sensor networks," in *Proc. IEEE 38th Annu. Conf. Local Comput. Netw. (LCN)*, Oct. 2013, pp. 219–227.

[11] J. Park, J. Jeong, H. Jeong, C.-J. Liang, and J. Ko, "Improving the packet delivery performance for concurrent packet transmissions in WSNs," *IEEE Commun. Lett.*, vol. 18, no. 1, pp. 58–61, Jan. 2014.

[12] D. Wu, C. Dong, S. Tang, H. Dai, and G. Chen, "Fast and fine-grained counting and identification via constructive interference in WSNs," in *Proc. ACM/IEEE IPSN*, Apr. 2014, pp. 191–202.

[13] M. Suzuki, Y. Yamashita, and H. Morikawa, "Low-power, end-to-end reliable collection using glossy for wireless sensor networks," in *Proc. IEEE 77th VTC Spring Conf.*, Jun. 2013, pp. 1–5.

[14] D. Carlson, M. Chang, A. Terzis, Y. Chen, and O. Gnawali, "Forwarder selection in multi-transmitter networks," in *Proc. IEEE DCOSS*, May 2013, pp. 1–10.

[15] *Texas Instruments CC2530*. Accessed: Jan. 31, 2018. [Online]. Available: http://www.ti.com/product/cc2530

[16] B. Bloessl, C. Leitner, F. Dressler, and C. Sommer, "A GNU radio-based IEEE 802.15.4 testbed," in *Proc. FGSN*, Cottbus, Germany, Sep. 2013, pp. 37–40.

[17] J. Lu and K. Whitehouse, "Flash flooding: Exploiting the capture effect for rapid flooding in wireless sensor networks," in *Proc. INFOCOM*, Apr. 2009, pp. 2491–2499.

[18] D. Son, B. Krishnamachari, and J. Heidemann, "Experimental study of concurrent transmission in wireless sensor networks," in *Proc. ACM SenSys*, New York, NY, USA, Oct. 2006, p. 237.

[19] M. Wilhelm, V. Lenders, and J. B. Schmitt, "On the reception of concurrent transmissions in wireless sensor networks," *IEEE Trans. Wireless Commun.*, vol. 13, no. 12, pp. 6756–6767, Dec. 2014.

[20] F. Hermans, H. Wennerström, L. McNamara, C. Rohner, and P. Gunningberg, "All is not lost: Understanding and exploiting packet corruption in outdoor sensor networks," in *Proc. Eur. Conf. Wireless Sensor Netw.* Cham, Switzerland: Springer, 2014, pp. 116–132.

[21] C. Sarkar. (2016). "LWB and FS-LWB implementation for sky platform using contiki." [Online]. Available: https://arxiv.org/abs/1607.06622

[22] *iMinds Technical Testing: iLab.t*. Accessed: Sep. 25, 2016. [Online]. Available: http://ilabt.iminds.be/

[23] M. Doddavenkatappa, M. C. Chan, and A. L. Ananda, "Indriya: A low-cost, 3D wireless sensor network testbed," in *Proc. Int. Conf. Testbeds Res. Infrastruct.* Berlin, Germany: Springer, 2011, pp. 302–316.

Vijay S. Rao received the bachelor's degree (Hons.) in computer science from VTU, India, in 2004, and the Ph.D. and M.Sc. degrees *(cum laude)* in telecommunication from the Delft University of Technology (TU Delft), The Netherlands, in 2017 and 2009, respectively. Since 2016, he has been a Post-Doctoral Fellow with the ENSys Group, Delft University of Technology. From 2004 to 2007, he was a Senior Software Engineer with ESQUBE Communications, Bengaluru, India, where he was involved in VoIP. He is also the Lead Developer for the TU Delft's rover (Zebro) for the moon. His research interests are in the Internet of Things, 5G, and tactile Internet. He has several peer-reviewed publications in the areas of WSNs, IoT, and VoIP. He holds two patents. He is a reviewer for several top-tier conferences and journals and has contributed to IEEE P1918.1 and P1906.1 standards.

R. Venkatesha Prasad is currently an Assistant Professor with the ENSys Group, Delft University of Technology. He has supervised 18 Ph.D. students and more than 40 M.Sc. students. He has participated in several European and Dutch projects in the areas of IoTs, 60-GHz communications, personal networks, and cognitive radios. He has around 250 publications in the peer-reviewed international journals and conferences. His research interests are in the area of tactile Internet, the Internet of Things, and 60-GHz MMW networks. He is a Senior Member of the IEEE and the ACM. He has served on the editorial boards of many IEEE Transactions. He was the Vice-Chair of the IEEE Tactile Internet Standardization Group. He is selected as the IEEE ComSoc Distinguished Lecturer on IoT for the period 2016–2018. He has contributed to several standards, including IEEE P1918.1 and P1906.1.

T. V. Prabhakar received the M.Sc. degree in physics and the M.Sc. (Engg.) and Ph.D. degrees. He is currently a Principal Research Scientist with Indian Institute of Science (IISc). He works in the area of networked embedded systems where he focuses on hardware system design, microenergy harvesting systems, and power management algorithms. He leads the effort in the Zero Energy Networks Laboratory, DESE, IISc, where his Ph.D. and master's students, project associates, and interns work on building embedded electronic systems for application areas, such as airplane cabin, industrial IoT, air quality, tactile Internet applications, autonomous drone charging systems, machine learning, and AI for IoT applications. Another focus area of his laboratory is related to object localization algorithms for RFID and IMU sensors. His laboratory has published over 50 papers in the IEEE and ACM conferences. The laboratory has received several best paper awards and showcased a few prototypes to the prime minister in the Startup India event organized by the Government of India in 2016.

Chayan Sarkar received the bachelor's degree from Jadavpur University in 2009, the master's degree in computer science from IIT Bombay in 2011, and the Ph.D. degree from the Delft University of Technology, The Netherlands, in 2016. He was a Post-Doctoral Scholar with SICS Swedish ICT, Sweden. He is currently a Scientist with TCS Research and Innovation, where he is currently part of the embedded systems and robotics research. His research interests include the Internet of Things, embedded systems, multi-robot systems, and human–robot interactions. He is part of the Organizing Committee of the IEEE ANTS and AIoTAS in 2017 and 2018 apart from serving as a reviewer for various conferences and journals.

Madhusudan Koppal received the bachelor's degree in electronics and communication engineering from VTU, India, in 2012. He was a Research Assistant under Dr. T. V. Prabhakar in DESE, Indian Institute of Science, India, from 2014 to 2016. He was an Engineer with HCL Technologies, India, from 2016 to 2018. He is currently an Engineer with Continental AG, India, working as an Automotive Embedded Software Developer.

Ignas Niemegeers received the M.Sc. degree in electrical engineering from the University of Gent, Belgium, in 1970, and the M.Sc. Ph.D. degrees in computer engineering from Purdue University, USA, in 1972 and 1978, respectively. From 1978 to 1981, he was a Designer of one of the first commercial packet switching networks with Bell Telephone Mfg. Cy, Antwerp, Belgium. From 1981 to 2002, he was a Professor with the University of Twente, The Netherlands. From 1995 to 2002, he was a Scientific Director with the Centre for Telematics and Information Technology, University of Twente. From 2002 to 2012, he chaired the Telecommunications Department, Delft University of Technology. He was involved in many European research projects and was a reviewer for many projects. He has supervised 42 Ph.D. students and has authored or coauthored around 300 papers. Since 2012, he has been the Emeritus Professor with the Delft University of Technology and an Advisor with the Centre for Wireless Technology, Eindhoven University of Technology, The Netherlands. Since 2016, he has been holding a part-time Chair in future optically supported wireless networks at the Eindhoven University of Technology. His current research interests are machine learning in radio access network architectures, radio-over-fiber, mmWave technologies, energy-harvesting IoT, and V2X communication.